Journal Name

COMMUNICATION

Graphene oxide - upconversion nanoparticle based optical sensors for targeted detection of mRNA biomarkers present in Alzheimer's disease and prostate cancer

Received 00th January 20xx,
Accepted 00th January 20xx

DOI: 10.1039/x0xx00000x

www.rsc.org/

Patrick Vilela,[a] Afaf El-Sagheer,[c,d] Timothy Millar,[e] Tom Brown,[c] Otto L. Muskens,[a,b] and Antonios G. Kanaras[a,b,*]

The development of new sensors for the accurate detection of biomarkers in biological fluids is of ultmost importance for the early diagnosis of diseases. Next to advanced laboratory techniques, there is a need for relatively simple methods which can significantly broaden the availability of diagnostic capability. Here, we demonstrate the successful application of a sensor platform based on graphene oxide and upconversion nanoparticles (NPs) to the specific detection of mRNA-related oligonucleotide markers in complex biological fluids. The combination of near-infrared light upconversion with low-background photon counting readout enables reliable detection of low quantities of small oligonucleotide sequences in the femtomolar range. We demonstrate the successful detection of analytes relevant to mRNAs present in Alzheimer's disease as well as prostate cancer in blood serum. The high performance and relative simplicity of the upconversion NP-graphene sensor platform enables new opportunities in early diagnosis based on specific detection of oligonucleotide sequences in complex environments.

Introduction

Messenger RNAs (mRNAs) are biomolecules which convey the necessary information for the ribosomal synthesis of proteins.[1] The detection of intracellular mRNA levels is of high importance for the monitoring of the progression of diseases[2-4], development of targeted drug treatments[5, 6] and onset diagnosis of disorders[7,8]. Several methods are available to detect the presence of specific mRNAs, such as Northern blotting, RNase Protection Assay, DNA microarrays and in situ hybridization.[9-12] For more sensitive studies of mRNA expression, real-time reverse-transcription quantitative polymerase chain reaction (RT-qPCR) is considered the standard protocol capable of quantifying RNA content from a volume as small as a single cell.[13] While these techniques are powerful tools for the research laboratory, the level of technical skill and specialist equipment required in preparation and analysis protocols often poses a disadvantage, limiting the widespread availability of such methods. Recently, a variety of sensors have been developed which based on the Förster resonance energy transfer (FRET) effect.[14-19] The sensitivity of these sensors is highly dependent on the efficiency of the fluorophore donor. Commonly used dyes have several drawbacks, including photo-bleaching, blinking effects and interferences from biomolecules in samples that absorb in the UV-Vis range, usually overlapping with the absorption regions of most common dyes.[20]

To overcome these issues, upconversion nanoparticles (UCNPs) have been developed as an alternative fluorescence donor. UCNPs are lanthanide-doped nanoparticles, which are able to absorb two or more low energy photons and emit fluorescence at a shorter wavelength than the excitation wavelength. Typically, UCNPs absorb in the near-infrared (NIR) region and emit in the visible region of the electromagnetic spectrum.[21] Additionally, UCNPs have shown great chemical and photochemical stability, low toxicity and absence of photo-bleaching or blinking effects.[22-24] When considering possible candidates for energy transfer acceptors, graphene oxide (GO) appears to be ideal, due to its high solubility in water[25], high surface area and efficient quenching[25, 26] and its characteristic affinity to various biomolecules.[27] For example, single stranded oligonucleotides are preferentially adsorbed to

[a] Physics and Astronomy, Faculty of Physical Sciences and Engineering
[b] Institute of Life Sciences, University of Southampton, Southampton, SO171BJ, UK. E-mail: A.Kanaras@soton.ac.uk
[c] Department of Chemistry, University of Oxford, Chemistry Research Laboratory, 12 Mansfield Road, Oxford, OX1 3TA, UK.
[d] Chemistry Branch, Department of Science and Mathematics, Faculty of Petroleum and Mining Engineering, Suez University, Suez 43721, Egypt.
[e] Faculty of Medicine, University of Southampton, Southampton, SO16 6YD, UK.
Electronic Supplementary Information (ESI) available: Design of DNA sequences, materials characterization, calibration experiments. A raw data file is also available at DOI:

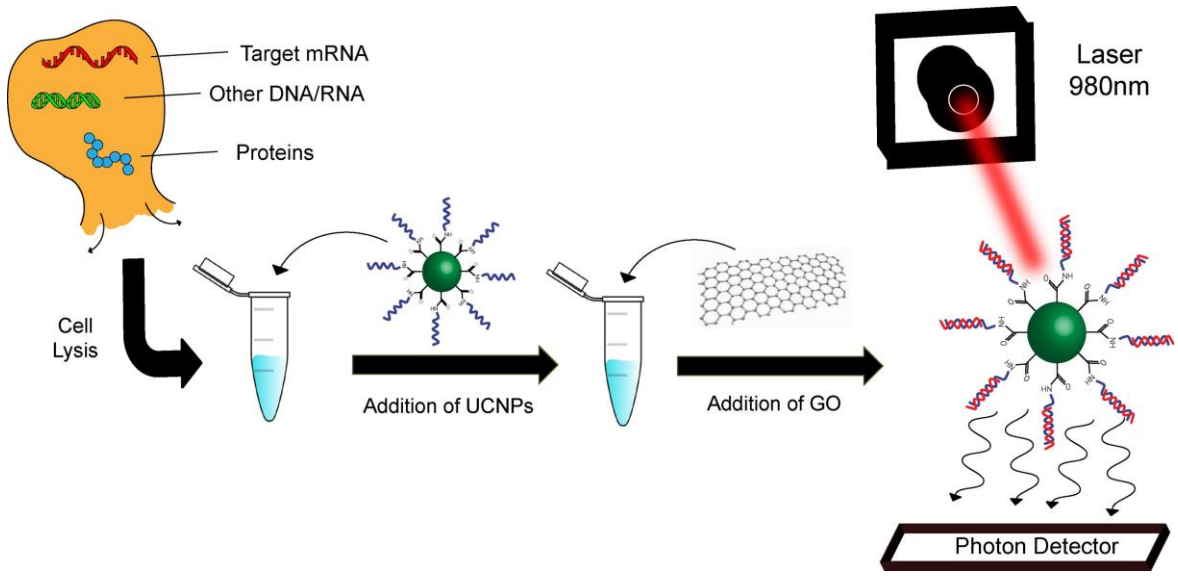

Scheme 1. Schematic route used for detection of biomarkers present in biopsy tissue or harvested cells. After lysis of the cells or tissue to be analysed, the obtained lysate is mixed firstly with the UCNPs coated with a sequence complementary to the target of interest. Then, the graphene oxide solution is added and the sample is irradiated with a laser at 980nm. Monitoring of the fluorescent signature of the particles concludes to the presence of the target sequence or not.

GO via π-π stacking interactions, whereas double stranded oligonucleotides do not bind.[28]. Recently, our group developed a sensor based on graphene oxide and upconversion nanoparticles to detect small poly-A sequences with the detection limit in the picomolar range (see ESI **Scheme S1**).[29] Here, we show for the first time the applicability of upconversion nanoparticle/graphene oxide sensors for the detection of mRNA-related biomarkers. We have selected the mRNA biomarker BACE-1 related to Alzheimer's disease[30] and the mRNA biomarker PCA3 related to prostate cancer[31-33] to demonstrate the applicability of the technique relevant for early detection of critical diseases. By using a single-photon counting detection scheme, we achieve a detection sensitivity of target oligonucleotide sequences down to the femtomolar range. Most importantly our sensors retain their sensitivity and selectivity in complex biological fluids such as blood plasma and cell lysate. A schematic illustration of the function of the sensors is shown in **Scheme 1**. A complex environment such as whole cell lysate is used as the starting solution to which UCNPs and GO are subsequently added in a two-step process. In the presence of BACE-1 or PCA3 target sequences, hybridization of the nucleotide chain results in a reduced adsorption of the UCNPs to the GO, which is subsequently detected by the fluorescent signature of the upconversion nanoparticles mediated by a 980 nm laser.

Results and Discussion

Synthesis and functionalization of upconversion nanoparticles

The synthesis of NaYF4:Yb,Er nanoparticles was done following a previously established procedure.[34, 35] The particles were monodisperse with a mean diameter of 27 ± 2 nm (see TEM image analysis in ESI **Figures S1A and S1B**). The synthesized particles had a characteristic fluorescence signature relevant to their composition (ESI **Figures S1C and S1D**). As synthesized nanoparticles were coated with oleic acid (OA) and dissolved in non-polar solvents. In order to transfer these particles in water, a ligand exchange reaction with polyacrylic acid (PAA) was performed following a simple substitution method.[36] The advantages of this method are that the particles can easily transfer in water and that the ligand shell contains several carboxylic groups, which can be further reacted via coupling reactions (ESI **Scheme S2**).

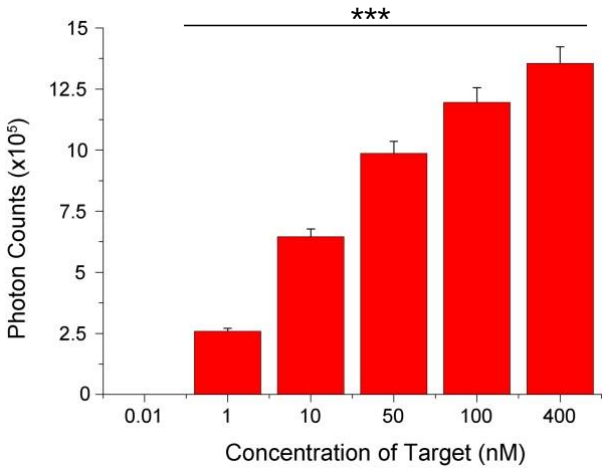

Figure 1. Detection of 545nm emitted photons from oligonucleotide coated UCNPs in the presence of GO (0.5 mg.mL-1) and different concentrations of the target sequence poly-A (***p<0.001). The detection of the target is directly proportional to the amount of target present in solution.

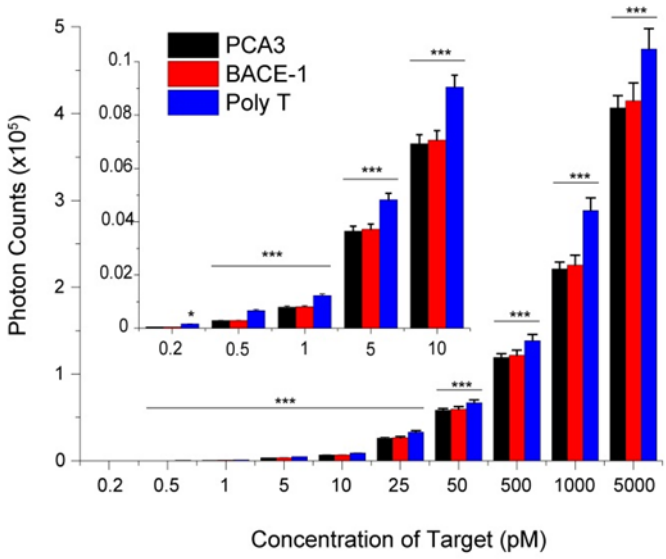

Figure 2. Performance of the sensors for the three oligonucleotide sense sequences (PCA3 (black), BACE-1 (red) and poly-T (blue) in PBS buffer (*p<0.01; ***p<0.001). An inset shows a magnification of the target detection for the range of 0.2-10 pM.

For the purpose of our experiments, amine-functionalized oligonucleotides were attached to the carboxylic groups of the nanoparticles via EDC/sulfo-NHS coupling. Three different oligonucleotide strands were employed. Two sense strands were designed to target selected areas of two mRNAs involved to Alzheimer disease (BACE-1) and prostate cancer (PCA3) (ESI **Table S1**). A third, nonspecific strand containing a poly-T sequence was designed as a general sequence that can detect the poly-A tail of any mRNA. The covalent binding of the oligonucleotides to the nanoparticle polymer shell was confirmed with ζ-Potential and UV-vis spectroscopy. Upon attachment of the sense strands to the nanoparticles, the zeta potential changed to a more negative value for all three types of oligonucleotides. This shift indicated the binding of the highly negative oligonucleotide strands to the nanoparticles (see ESI **Figure S2A**). The presence of oligonucleotides on the nanoparticle's surface was also confirmed with the appearance of a 280 nm peak on the UV spectra (ESI **Figure S2B**). The resulting oligonucleotide coated UCNPs were very stable and showed the characteristic Er-upconversion fluorescence spectrum under excitation with light from a 980 nm wavelength laser source (**Figure 1**).

Targeting specificity and calculation of the detection limit

Calibration of the sensors was achieved by adding different concentrations of graphene oxide ranging from 0 to 1 mg.mL^{-1} to a fixed concentration of oligonucleotide coated upconversion nanoparticles (0.5 mg.mL^{-1}). The photon counts decreased proportionally with increasing concentrations of GO (ESI **Figure S3**). The lowest concentration of GO that achieves the highest degree of quenching was determined to be 0.5 mg.mL^{-1}. To test the stability of the sensor we monitored its performance over a period of 30 days (ESI **Figure S4**). It was observed that there were no significant variations on the values obtained, demonstrating the high stability of the sensor. Three different batches of oligonucleotide coated UCNPs were synthesised

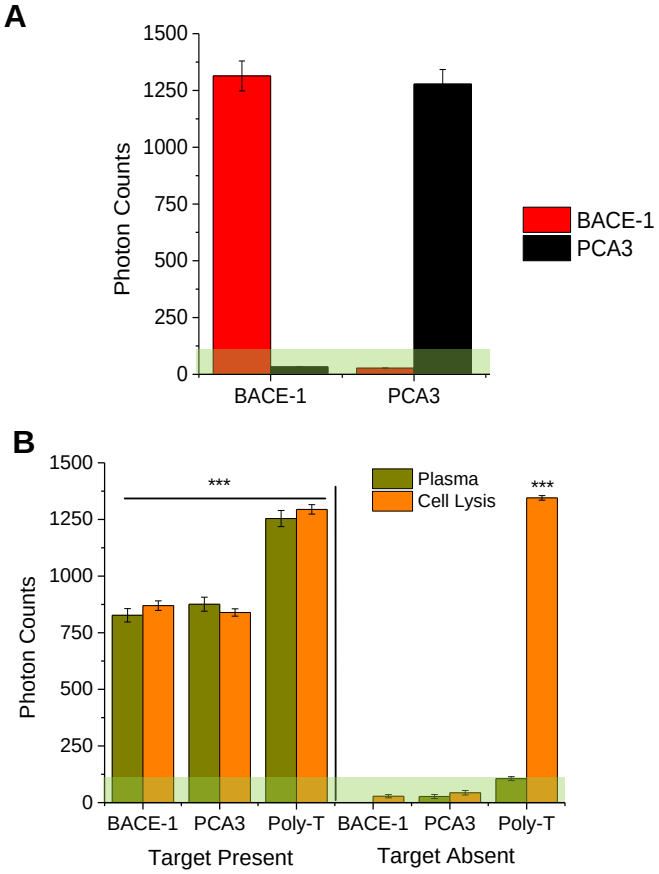

Figure 3. A) Specific oligonucleotide detection by the sensors in a cocktail of both BACE-1 and PCA3 targets (***p<0.001) in PBS. B) Performance of the sensors in the presence and absent of the relevant oligonucleotide targets in plasma (dark green) and cell lysis (orange). At the absence of the target, the poly-T sensor is able to detect the poly-A tails of all mRNAs in cell lysis (***p<0.001). The noise limit is represented by the light green area.

using sequences for the detection of Poly-A tails, BACE-1 and PCA3 (ESI Table S1). Each batch was incubated with the respective target sequence. **Figure 2** shows the detection of the targets for various concentrations. The detection limit for every target was directly proportional to the concentrations of the respective sequence. It was possible to observe that the lowest experimental detection limit for poly-A was 200 fM and for the other two targets was 500 fM (ESI **Figure S5**), since those concentrations were significantly above the detection limit threshold.

Selectivity of the sensor and function in blood plasma and cell lysis

An important aspect of a sensor is their ability to selectively detect a target in challenging environments, where biomolecules such as

proteins and non-specific mRNAs could interfere with the detection of the target mRNA biomarkers**.**

The selectivity of our sensors was tested by subjecting them to both BACE-1 and PCA3 target oligonucleotide sequences at the same time. **Figure 3A** shows photon counts for BACE-1 (red) and PCA3 (black) sensors, when exposed to these oligonucleotide sequences. The results show that the sensors are highly selective without interfering with other sequences other than the respective target. Subsequently, we tested the sensors both in whole cell lysate and in blood plasma, where in each medium the specific target was either present or absent. **Figure 3B** shows the performance of the sensors in these media.

In comparison to the Alzheimer and prostate cancer sensors, which did not show a detection response in absence of the target sequence either in plasma or cell lysis media, the poly-T oligonucleotide sequence sensor gave a strong fluorescent signal in the absence of the poly-A sequence in cell lysis medium. This observation is attributed to the presence of multiple mRNAs in the cell lysis that carry a poly-A tail, which is detectable by the poly-T sensor, highlighting the excellent performance of the sensor for general mRNA targeting.

Conclusions

In summary, we successfully designed graphene oxide/upconversion nanoparticle sensors capable of detecting oligonucleotides sequences relevant to mRNA sequences associated with Alzheimer disease and prostate cancer. Our sensors have several important advantages when compared with previously reported systems. They are highly sensitive with a detection limit in the femtomolar range and with no drawbacks related to photo-blinking or biomolecule absorbance interferences. We have demonstrated that the sensor platform is highly selective to a specific target mRNA even in complex media such as blood plasma and cell lysate where the interference from other biomolecules is significant. These sensors will be of broad interest as mRNA biomarkers in early diagnosis of critical diseases such as Alzheimer's disease and prostate cancer.

References

1. C. H. Contag and M. H. Bachmann, *Annu Rev Biomed Eng*, 2002, **4**, 235-260.
2. T. R. Golub, D. K. Slonim, P. Tamayo, C. Huard, M. Gaasenbeek, J. P. Mesirov, H. Coller, M. L. Loh, J. R. Downing, M. A. Caligiuri, C. D. Bloomfield and E. S. Lander, *Science*, 1999, **286**, 531-537.
3. D. G. Beer, S. L. R. Kardia, C. C. Huang, T. J. Giordano, A. M. Levin, D. E. Misek, L. Lin, G. A. Chen, T. G. Gharib, D. G. Thomas, M. L. Lizyness, R. Kuick, S. Hayasaka, J. M. G. Taylor, M. D. Iannettoni, M. B. Orringer and S. Hanash, *Nat Med*, 2002, **8**, 816-824.
4. H. Y. Chang, J. B. Sneddon, A. A. Alizadeh, R. Sood, R. B. West, K. Montgomery, J. T. Chi, M. van de Rijn, D. Botstein and P. O. Brown, *Plos Biol*, 2004, **2**, 206-214.
5. J. P. Hughes, S. Rees, S. B. Kalindjian and K. L. Philpott, *Brit J Pharmacol*, 2011, **162**, 1239-1249.
6. U. Sahin, K. Kariko and O. Tureci, *Nat Rev Drug Discov*, 2014, **13**, 759-780.
7. C. P. Pipinikas, N. D. Carter, C. M. Corbishley and C. D. Fenske, *Biomarkers*, 2008, **13**, 680-691.
8. C. F. Ng, R. Yeung, P. K. Chiu, N. Y. Lam, J. Chow and B. Chan, *Hong Kong Med J*, 2012, **18**, 459-465.
9. S. Streit, C. W. Michalski, M. Erkan, J. Kleeff and H. Friess, *Nat Protoc*, 2009, **4**, 37-43.
10. F. Katagiri and J. Glazebrook, *Curr Protoc Mol Biol*, 2009, **Chapter 22**, Unit 22 24.
11. P. B. Brewer, M. G. Heisler, J. Hejatko, J. Friml and E. Benkova, *Nat Protoc*, 2006, **1**, 1462-1467.
12. E. Stylianopoulou, D. Lykidis, P. Ypsilantis, C. Simopoulos, G. Skavdis and M. Grigoriou, *PLoS One*, 2012, **7**, e33898.
13. M. L. Wong and J. F. Medrano, *Biotechniques*, 2005, **39**, 75-85.
14. C. Y. Zhang, H. C. Yeh, M. T. Kuroki and T. H. Wang, *Nat Mater*, 2005, **4**, 826-831.
15. N. C. Cady, A. D. Strickland and C. A. Batt, *Molecular and cellular probes*, 2007, **21**, 116-124.
16. M. Suzuki, Y. Husimi, H. Komatsu, K. Suzuki and K. T. Douglas, *J Am Chem Soc*, 2008, **130**, 5720-5725.
17. K. Lee, J. M. Rouillard, B. G. Kim, E. Gulari and J. Kim, *Adv Funct Mater*, 2009, **19**, 3317-3325.
18. L. Gao, C. Lian, Y. Zhou, L. Yan, Q. Li, C. Zhang, L. Chen and K. Chen, *Biosens Bioelectron*, 2014, **60**, 22-29.
19. J. Y. Shi, F. Tian, J. Lyu and M. Yang, *J Mater Chem B*, 2015, **3**, 6989-7005.
20. A. M. Smith and S. M. Nie, *Accounts Chem Res*, 2010, **43**, 190-200.
21. M. Haase and H. Schafer, *Angew Chem Int Ed Engl*, 2011, **50**, 5808-5829.
22. C. T. Xu, P. Svenmarker, H. C. Liu, X. Wu, M. E. Messing, L. R. Wallenberg and S. Andersson-Engels, *Acs Nano*, 2012, **6**, 4788-4795.
23. Y. F. Wang, G. Y. Liu, L. D. Sun, J. W. Xiao, J. C. Zhou and C. H. Yan, *Acs Nano*, 2013, **7**, 7200-7206.
24. F. Chen, W. B. Bu, S. J. Zhang, J. N. Liu, W. P. Fan, L. P. Zhou, W. J. Peng and J. L. Shi, *Adv Funct Mater*, 2013, **23**, 298-307.
25. C. H. Lu, H. H. Yang, C. L. Zhu, X. Chen and G. N. Chen, *Angew Chem Int Ed Engl*, 2009, **48**, 4785-4787.
26. S. H. Li, A. N. Aphale, I. G. Macwan, P. K. Patra, W. G. Gonzalez, J. Miksovska and R. M. Leblanc, *ACS applied materials & interfaces*, 2012, **4**, 7068-7074.
27. M. Wu, R. Kempaiah, P. J. Huang, V. Maheshwari and J. Liu, *Langmuir*, 2011, **27**, 2731-2738.
28. J. S. Park, N. I. Goo and D. E. Kim, *Langmuir*, 2014, **30**, 12587-12595.
29. P. Alonso-Cristobal, P. Vilela, A. El-Sagheer, E. Lopez-Cabarcos, T. Brown, O. L. Muskens, J. Rubio-Retama and A. G. Kanaras, *ACS applied materials & interfaces*, 2015, **7**, 12422-12429.
30. H. W. Querfurth and F. M. LaFerla, *New Engl J Med*, 2010, **362**, 329-344.

31. J. B. de Kok, G. W. Verhaegh, R. W. Roelofs, D. Hessels, L. A. Kiemeney, T. W. Aalders, D. W. Swinkels and J. A. Schalken, *Cancer Res*, 2002, **62**, 2695-2698.
32. L. S. Marks and D. G. Bostwick, *Rev Urol*, 2008, **10**, 175-181.
33. E. D. Crawford, K. O. Rove, E. J. Trabulsi, J. Q. Qian, K. P. Drewnowska, J. C. Kaminetsky, T. K. Huisman, M. L. Bilowus, S. J. Freedman, W. L. Glover and D. G. Bostwick, *J Urology*, 2012, **188**, 1726-1731.
34. Z. Q. Li and Y. Zhang, *Nanotechnology*, 2008, **19**.
35. C. Liu, H. Wang, X. Li and D. Chen, *J Mater Chem*, 2009, **19**, 3546-3553.
36. W. Lin, K. Fritz, G. Guerin, G. R. Bardajee, S. Hinds, V. Sukhovatkin, E. H. Sargent, G. D. Scholes and M. A. Winnik, *Langmuir*, 2008, **24**, 8215-8219.